Available online at www.sciencedirect.com
ScienceDirect
C. R. Mecanique 336 (2008) 363–369
COMPTES RENDUS MECANIQUE
http://france.elsevier.com/direct/CRAS2B/

3D coherent vortices in the turbulent near wake of a square cylinder

Christophe Brun [a,b,*], Thomas Goossens [b]

[a] *L.E.G.I., BP. 53, 38041 Grenoble cedex 09, France*
[b] *L.M.E., 8, rue Léonard-de-Vinci, 45000 Orléans, France*

Received 7 December 2007; accepted after revision 13 December 2007

Available online 20 February 2008

Presented by Marcel Lesieur

Abstract

Large Eddy Simulations of a constant-density flow carrying a passive scalar around a square cylinder at Reynolds numbers $Re = 1000$ and $Re = 1500$ are performed. We describe the three-dimensional topology of the turbulent flow in terms of intense longitudinal counter-rotating coherent vortices. We show also a change of regime concerning spanwise Kelvin–Helmholtz (KH) vortices. At the lower Reynolds number, they roll up downstream of the obstacle to form the von Kármán vortex street (VK). At higher Reynolds, they form immediately in the separating shear layer on the two sides of the cylinder. The role of vortices in the passive-scalar mixing is also looked at. ***To cite this article: C. Brun, T. Goossens, C. R. Mecanique 336 (2008).***

Résumé

Tourbillons cohérents 3D dans le proche sillage turbulent d'un cylindre à section carrée. Nous présentons des résultats de Simulations des Grandes Echelles d'un écoulement de densité uniforme transportant un scalaire passif autour d'un cylindre de section carrée à nombre de Reynolds $Re = 1000$ et $Re = 1500$. Nous décrivons la topologie tri-dimensionnelle de l'écoulement turbulent sous forme de tourbillons cohérents longitudinaux intenses contrarotatifs. Nous montrons aussi un changement de régime affectant les tourbillons de Kelvin–Helmholtz (KH) transverses. A bas Reynolds, ils se forment en aval de l'obstacle pour constituer l'allée de von Kármán (VK). A haut Reynolds, ils se forment immédiatement dans la couche cisaillée décollée sur les deux parois du cylindre. Le rôle des tourbillons dans le mélange du scalaire passif est aussi étudié. ***Pour citer cet article : C. Brun, T. Goossens, C. R. Mecanique 336 (2008).***

Keywords: Computational fluid mechanics; Large Eddy Simulation; Turbulence; Cylinder wake; Streamwise vortices; Passive-scalar mixing

Mots-clés : Mécanique des fluides numérique ; Simulation des Grandes Echelles ; Turbulence ; Sillage de cylindre ; Tourbillons longitudinaux ; Mélange de scalaire passif

* Corresponding author.
E-mail address: christophe.brun@hmg.inpg.fr (C. Brun).

1631-0721/$ – see front matter
doi:10.1016/j.crme.2008.01.002

1. Introduction

The analysis of turbulent flow behind a cylinder is of great practical interest since it constitutes a generic configuration with many applications in fields such as nuclear engineering, external aerodynamics and environmental sciences. As an example, mixing properties in heat exchangers play a key role in thermal hydraulic problems related to powerplants. Another example is the reduction of aeroacoustics sources generated by rearview mirror in car design. A third direct application is the scalar diffusion around buildings and the effect on atmospheric pollution mixing. There exists indeed a non-exhaustive list of practical applications in the field of both engineering and geophysical flows where turbulent wakes interact strongly with the integral scales of the problem to tackle.

In the present Note, we focus on the topological analysis of 3D coherent vortices which develop in the separated shear layer on the side of a square cylinder and coalesce downstream in the near wake behind the obstacle. A detailed analysis of such a flow based on both Large Eddy Simulations (LES) for $500 \leqslant Re \leqslant 2000$ and Laser Doppler Velocimetry for $20\,000 \leqslant Re \leqslant 300\,000$ is available elsewhere [1]. It is a study of the various specific time scales of the turbulent separating flow around the cylinder determined from wavelet analysis among other more classical statistical procedures. In the present note we perform LES of the turbulent flow around a square cylinder at $Re = 1000$ and $Re = 1500$ with passive-scalar transport in order to describe in details some topological 3D aspects which contribute to the mixing process of the flow. The present Reynolds number regime is slightly above the transitional regime for which Kelvin–Helmholtz (KH) instabilities develop on the top of Von Kármán (VK) instabilities in the near wake of a cylinder [2]. For a round cylinder, it was first shown by Wei and Smith [3] that *"immediately following their formation the vortices* (KH) *undergo a strong three-dimensional distortion, which may provide the mechanism for the transition to turbulent Strouhal vortices"* (VK). In the present case, a qualitative description of both the turbulent flow and the transport of a scalar shows the role of streamwise vortices development on the flow mixing properties. Such mixing process is specific to KH vortices dynamics in turbulent shear layers, and was already observed in LES of e.g. plane mixing layers [4], plane jets [5], incompressible and compressible round jets [6,7], and coaxial jets [8]. It was originally discussed in shear layer experiments [9–11].

2. Flow configuration and numerical method

LES of the turbulent flow around a square cylinder of diameter D have been performed on IDRIS high performance computer (IBM cluster with Regatta Power4 processors) using 1 to 5 million grid points (Table 1). A parallel version with 8 to 32 processors of the Trio_U code (CEA Grenoble) using MPI is used to solve the uniform density Navier–Stokes equations [12] including a transport equation for the temperature set as a passive scalar (constant fluid properties). The computation domain extends on $L_x^- = 3D$ upstream of the cylinder and on $L_x^+ = 10D$ behind the cylinder in the streamwise direction, on $L_y = 13D$ in the transverse direction and on $L_z = 8D$ in the spanwise direction. The discretization is a staggered finite volume method. Space derivatives are fourth-order centered for the convection. A third order Runge–Kutta scheme is used for time advancement. The pressure field is calculated using an SSOR conjugate gradient solver. A local grid refinement is applied close to the cylinder so that no wall treatment is necessary in the transverse y direction. The flow case with 32 processors is useful to reach a mesh size $\Delta z = 0.05D$ in the spanwise direction, smaller than the mesh size used in existing Direct Numerical Simulations (DNS) in the

Table 1
Flow configuration

Tableau 1
Paramètres des simulations

	Re	L_x	L_y	L_z	$n_x \times n_y \times nz$	processors nb
LES + scalar	1000	$14D$	$13D$	$8D$	$220 \times 175 \times 35$	8
LES + scalar	1500	$14D$	$13D$	$8D$	$220 \times 175 \times 35$	8
LES	1500	$14D$	$13D$	$8D$	$220 \times 175 \times 137$	32
DNS [13]	500	$22D$	$18D$	$6D$	$209 \times 129 \times 41$	–
DNS [14]	500	$24D$	$10D$	$6D$	$218 \times 104 \times 32$	–
LES [16]	21 400	$20D$	$12D$	$4D$	$274 \times 280 \times 50$	–
LES [15]	22 000	$22D$	$18D$	$6D$	$185 \times 105 \times 25$	–

literature for $Re = 500$ with $\Delta z = 0.15D$ [13] or $\Delta z = 0.20D$ [14], and other reference LES for $Re = 21\,400$ with $\Delta z = 0.167D$ [15] or $0.08D \leqslant \Delta z \leqslant 0.32D$ [16]. The present choice of discretization is coherent with the objective of the study to fully determine KH structures which are known to be $2D$ instabilities in the initial stage of their formation [17] and rapidly yield $3D$ vortices and transition to turbulence [3]. Thus, the present 32 processors case is almost a DNS in the neighbourhood of the cylinder, while it is a classical LES in the wake further downstream. The LES uses the Selective Structure Function [18] as SubGrid Scale (SGS) model. SGS diffusion for the scalar transport equation is modelled based on the classical assumption of constant SGS Prandtl number [19] $Pr_{\mathrm{SGS}} = 0.6$.

A uniform constant velocity U_o and a uniform constant temperature T_o are set as inflow conditions. Unlike the case of spatially developing turbulent boundary layers [20,21] or spatially developing turbulent shear layers [22,7] where the design of proper realistic turbulent inflow conditions is an issue, no superimposed noise was necessary in the present case. The main reason is that for the considered Reynolds number regime $Re = 1000$–1500, the boundary layer around the cylinder is laminar above the flow separation and gets turbulent in the separated shear layer downstream in the near-wake [17]. Indeed, the quasiperiodic flow property of the Kármán vortex street which is an hydrodynamic instability of absolute nature is enough to trigger the transition to turbulence which occurs in the separated shear layer. Outflow conditions consist of a free advection procedure [23] to extract both coherent vortices and passive tracers from the simulation domain. Free-slip boundary conditions are applied in the transverse and spanwise directions. No-slip velocity boundary condition and uniform constant temperature T_1 are set on the cylinder wall.

3. Results

Fig. 1 shows the turbulent flow in the near wake behind a square cylinder computed with the lowest resolved case (8 processors) for $Re = 1000$ and $Re = 1500$. The temperature distribution in the wake constitutes a useful scalar tracer for the turbulent flow description. Isovalues of temperature (colored in yellow) indicate that the large scale Kármán vortex street which consists of alternatively shedded vortex tubes from the top and the bottom of the cylinder take part to the mixing in a whole and tear an amount of scalar from the cylinder towards the wake. Temperature isovalues were set to $T = T_o + 0.2(T_1 - T_o)$ and it is clear that more scalar is brought to the flow for the case $Re = 1500$, related to a higher level of turbulence. Vorticity isovalues are useful to point out small scale vortices and intense turbulent regions. A well established way to visualize these small scales vortices is obtained based on the Q-criterion, a quantity which is related to the second invariant of the velocity gradient tensor [24]. Isovalues set to $Q = 0.4U_o^2/D^2$ indicate that the flow gets rapidly 3D in the near wake and yields intense streamwise vortices stretched between two 2D large vortex tubes. Such streamwise vortices were also observed in the wake of both round and square cylinders for higher Reynolds number regimes [17,25,26]. Blue and red colors are used to show the sign of these streamwise vortices which are further advected together and form dipoles structures known to be very intense. These vortices are much more aligned in the streamwise direction for the higher Reynolds number case $Re = 1500$ (Fig. 1(b)), while for

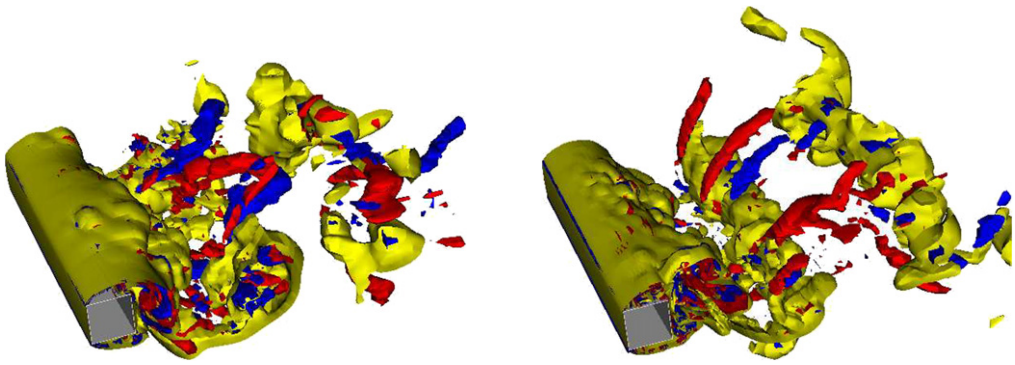

(a) $Re = 1000$ (b) $Re = 1500$

Fig. 1. Near wake behind a square cylinder (8 processors). Isovalues of the scalar field (yellow $T = T_o + 0.2(T_1 - T_o)$) and of the Q-criterion (green $Q = 0.4U_o^2/D^2$) colored by axial vorticity (red $\omega_x \geqslant 0$, blue $\omega_x \leqslant 0$).

Fig. 1. Proche sillage en aval d'un cylindre à section carrée (8 processeurs). Isovaleurs du champ de scalaire (jaune, $T = T_o + 0.2(T_1 - T_o)$) et isovaleurs du critère Q ($Q = 0.4U_o^2/D^2$) colorées par la vorticité axiale (rouge $\omega_x \geqslant 0$, bleu $\omega_x \leqslant 0$).

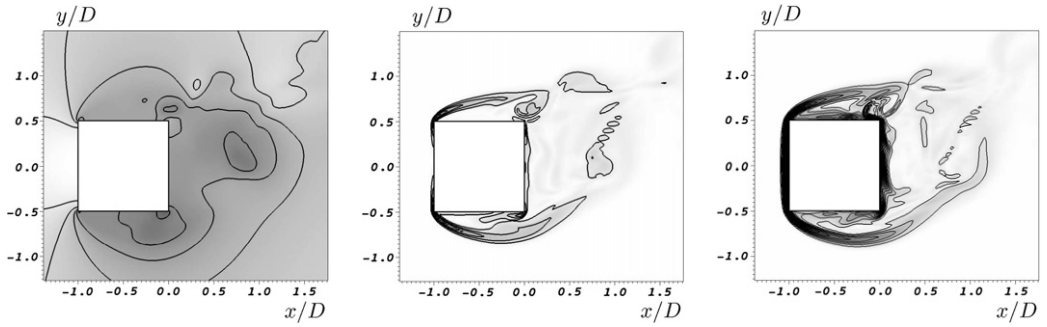

(a) Pressure for $Re = 1000$ (b) Vorticity for $Re = 1000$ (c) Scalar gradient for $Re = 1000$

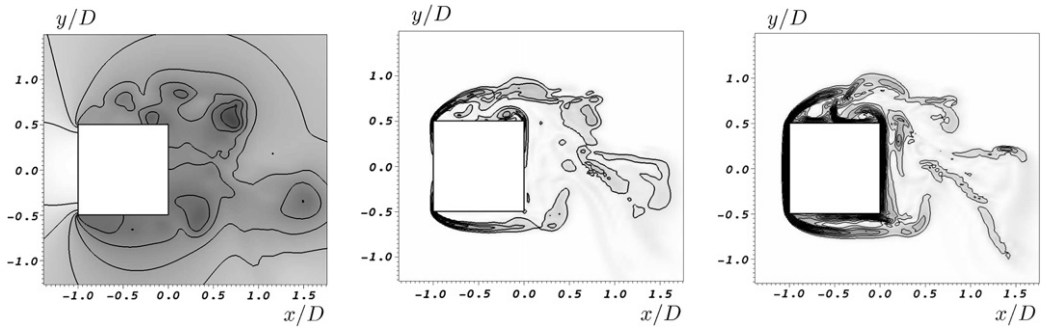

(d) Pressure for $Re = 1500$ (e) Vorticity for $Re = 1500$ (f) Scalar gradient for $Re = 1500$

Fig. 2. Slice of the flow around the square cylinder for pressure isovalues (a), (d), isovalues of the vorticity norm (b), (e) and temperature gradient isovalues (c), (f) for $Re = 1000$ and $Re = 1500$ (8 processors).

Fig. 2. Coupe de l'écoulement autour du cylindre à section carrée pour les isovaleurs de pression (a), (d), de la norme de vorticité (b), (e) et du gradient de température (c), (f) à $Re = 1000$ et $Re = 1500$ (8 processeurs).

$Re = 1000$ they still form a wavy spanwise structure (Fig. 1(a)). The distorsion of spanwise vortex tubes is much faster for increasing Reynolds number, which offers a strong argument in favour of the 3D mixing property enhancement.

It is well known since Bloor in 1964 [2] that for a round cylinder, "*transition to turbulence occurs before the separated layer rolls up in the wake ... and is observed at all Reynolds numbers larger than* $Re = 1300$". The threshold of the shear layer instability which leads to the development of KH vortices in the shear layers on the sides of a square cylinder is at about the same Reynolds number value [26,1]. Fig. 2 is a zoom of the flow in our simulation for the two Reynolds numbers $Re = 1000$ and $Re = 1500$ surrounding this threshold. Slices of respectively pressure, vorticity norm and scalar gradient isovalues are shown. Vortices are identified by pressure minima [27], maxima of vorticity versus strain [24] and scalar gradients extrema. The choice of the scalar gradient isosurface instead of the scalar itself is discussed in Lesieur, Métais and Comte [28] (p. 24): within a vortex, a quasi 2D analysis shows that the scalar gradient will rotate in the same way as a passive vector (whose rotation is implied by the Q-criterion). For $Re = 1000$, the shear layers on the top and the bottom of the cylinder remain stable and roll up behind the obstacle to form directly the first vortex of the Kármán street in the rear of the cylinder. For $Re = 1500$, KH vortices appear in the shear layer on the top of the cylinder and roll up further downstream in the large scale Kármán vortex street. Such a behaviour had already been observed numerically by Braza et al. [29] and experimentally by Kourta et al. [30] behind a circular cylinder. As a result, the scalar gradient is much more uniform for the lower Reynolds number case, and the mixing which can be measured by the spreading of the scalar gradient is much stronger for the higher Reynolds number case. Notice for the case $Re = 1500$ the ejection of fluid and scalar on the top of the cylinder from the wall to the upper boundary.

Fig. 3 shows isovalues of the Q-criterion (green: $Q = 5U_o^2/D^2$) in the separating shear layer on the side of the square cylinder for $Re = 1500$. The isovalue threshold is $Q = 0.3U_c^2/\delta_\omega^2$ with respect to the mean convection velocity in the shear layer $U_c = U_o/2$ and to the vorticity thickness $\delta_\omega = 0.12D$ evaluated at $x = -0.5D$ in the middle of the cylinder side wall [1]. We note that the normalized threshold has the same order of magnitude (about 0.5) when the right choice of normalization is made, that is to say with the large scales $[U_o, D]$ in the wake of the cylinder

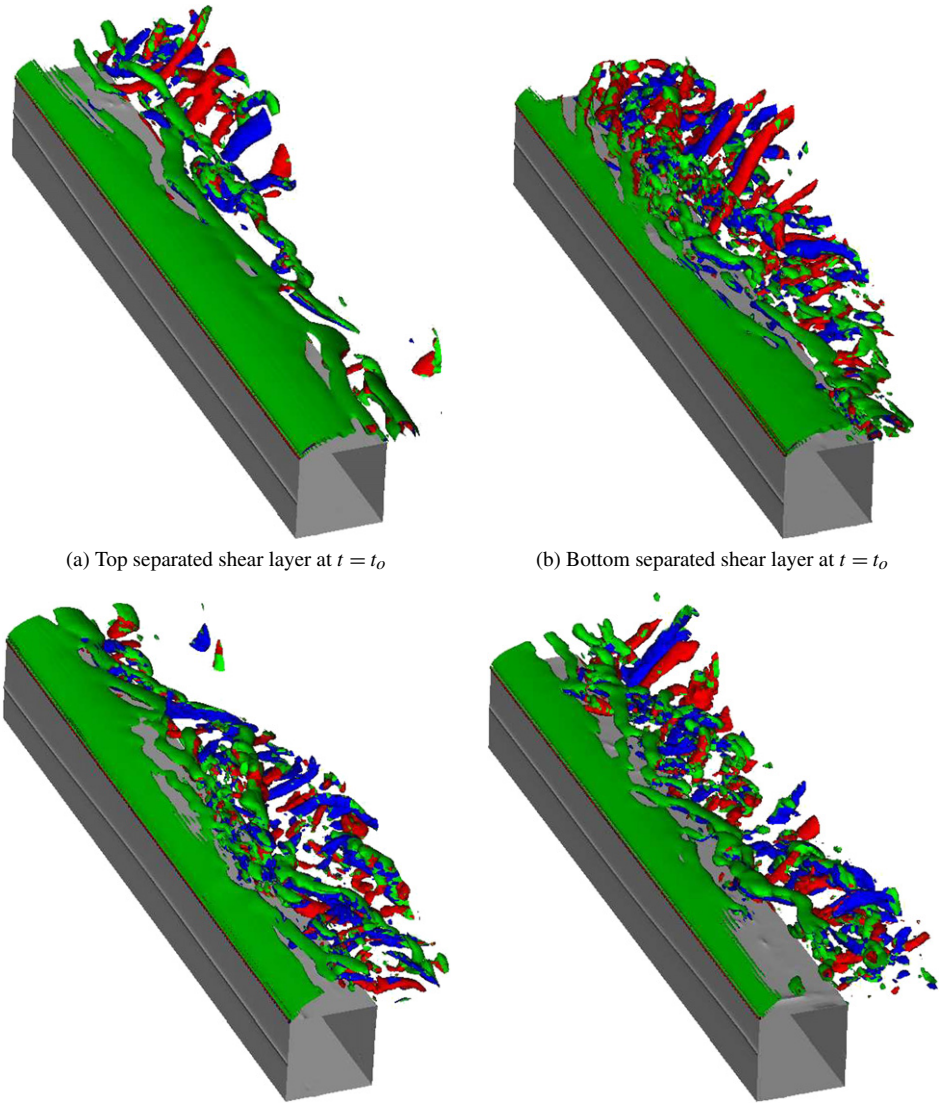

(a) Top separated shear layer at $t = t_o$

(b) Bottom separated shear layer at $t = t_o$

(c) Top separated shear layer at $t = t_o + 4.0D/U_o$

(d) Bottom separated shear layer at $t = t_o + 4.0D/U_o$

Fig. 3. Q-criterion isovalues (green $Q = 5U_o^2/D^2 = 0.3U_c^2/\delta_\omega^2$) colored by axial vorticity (red $\omega_x \geqslant 0$, blue $\omega_x \leqslant 0$) in the separated shear layer on top or bottom of a square cylinder for $Re = 1500$ (32 processors).

Fig. 3. Isovaleurs du Critère Q (vert $Q = 5U_o^2/D^2 = 0.3U_c^2/\delta_\omega^2$) colorées par la vorticité axiale (rouge $\omega_x \geqslant 0$, bleu $\omega_x \leqslant 0$) dans la couche cisaillée décollée au-dessus et en dessous d'un cylindre à section carrée à $Re = 1500$ (32 processeurs).

and with the intermediate scales $[U_c, \delta_\omega]$ in the separated shear layer. We present two decorrelated time samples, showing the small scale structures related to the local shear layer instability. Visualizations are performed on both the top side and the bottom side (after rotation of the reference axis) of the cylinder. Q isovalues are colored in red for $\omega_x \geqslant 0$ and in blue for $\omega_x \leqslant 0$ when the local axial vorticity level is sufficiently high with respect to a given threshold (about $\|\omega_x\| = 90\% Q^{1/2}$). First note the 2D initial behaviour of the shear layer instability near the upward separation point at the upper corner of the cylinder [31]. KH vortices tubes (colored in green) are first advected on the top of the cylinder. Second, the vortex tubes are stretched in the streamwise direction and form wavy spanwise structures [3,9,10]. Third, local pairings of the vortex tubes occur after 2∼3 KH sheddings. This yields a strong three-dimensionality of the flow related to the merging of KH vortex tubes. In the meantime intense streamwise longitudinal vortices appear, colored in blue and red according to the rotation direction. These streamwise vortices are numerous in the initial stage of transition to turbulence on the top of the cylinder (about a dozen of counter-rotating streamwise

vortices pairs along the spanwise $8D$ length of the cylinder). Further downstream of the cylinder, successive pairings lead to the configuration shown on Fig. 1(b) with about only four remaining streamwise vortices in the wake. The phenomenology of the flow is very similar indeed to what was observed for plane mixing layers [4], plane jets [5] or coaxial jets [8]. Mixing properties related to the present streamwise vortices in the cylinder near field are enhanced by the KH instability development in the separating shear layers around the cylinder.

4. Conclusions

We have performed LES of the turbulent flow around a square cylinder with transport of a passive scalar for $Re = 1000$ and $Re = 1500$, that is to say for two Reynolds number values surrounding the threshold $Re_c \approx 1300$ for which KH vortices develop in the separating shear layers on both the sides of the obstacle (study on a circular cylinder done in [2]). For the lower Reynolds number case, KH vortices roll up directly in the Kármán vortex street behind the cylinder to form the large scale spanwise vortex tubes which stretch hairpin streamwise vortex structures further downstream. For the higher Reynolds number case, a zoom of the topology of the turbulent flow in the separating shear layers shows that KH vortices which are initially quasi two-dimensional are rapidly subjected to 3D distorsion and yield intense and numerous longitudinal vortices which coalesce together and finally form dipoles of opposite vorticity sign. All these stages occur in a very short distance, about two diameters long, downstream of the cylinder and contribute to enhance transition to turbulence and passive-scalar diffusion. It is known for long that streamwise vortices exist in the near wake, even at lower Reynolds number for a circular cylinder [17]. But, to our knowledge, such 3D process applied to the longitudinal deformation of KH vortices in the shear layer zone on the side of the cylinder was only pointed out by Wei and Smith [3] based on experimental visualizations of the flow around a round cylinder in the Reynolds number range $1200 \leqslant Re \leqslant 11\,000$.

Acknowledgements

Computations were carried out at IDRIS (Institut du Développement et des Ressources en Informatique Scientifique, Orsay) with the Trio_U code developed at the CEA (Commissariat à l'énergie atomique Grenoble). The study was part of a DFG-CNRS research project UR 507, entitled 'LES of complex flows'.

References

[1] C. Brun, T. Goossens, S. Aubrun, P. Ravier, Coherent structures and their frequency signature in the separated shear layer on the sides of a square cylinder, Flow, Turbulence and Combustion (2008), in press.
[2] M.S. Bloor, The transition to turbulence in the wake of a circular cylinder, J. Fluid Mech. 19 (1964) 290.
[3] T. Wei, C.R. Smith, Secondary vortices in the wake of circular cylinders, J. Fluid Mech. 169 (1986) 513.
[4] P. Comte, J.H. Silvestrini, P. Bégou, Streamwise vortices in large-eddy simulations of mixing layers, Eur. J. Mech. B/Fluids 17 (4) (1998) 615–637.
[5] C.B. da Silva, O. Métais, On the influence of coherent structures upon interscale interactions in turbulent plane jets, J. Fluid Mech. 473 (2002) 103–145.
[6] C.B. da Silva, O. Métais, Vortex control of bifurcating jets: a numerical study, Phys. Fluids 14 (1) (2002) 3798–3819.
[7] M. Maidi, Estimation of aerodynamic noise generated by forced compressible round jets, C. R. Mecanique 334 (2006) 285–291.
[8] G. Balarac, M. Si Ameur, Mixing and coherent vortices in turbulent coaxial jets, C. R. Mecanique 333 (2005) 622–627.
[9] L.P. Bernal, A. Roshko, Streamwise vortex structure in plane mixing layers, J. Fluid Mech. 170 (1986) 499–525.
[10] J.C. Lasheras, J.S. Cho, T. Maxworthy, The origin and evolution of streamwise vortical structures in a plane, free shear layer, J. Fluid Mech. 172 (1986) 231–258.
[11] D. Liepmann, M. Gharib, The role of streamwise vorticity in the near-field entrainment of round jets, J. Fluid Mech. 245 (1992) 643–668.
[12] R.J.A. Howard, M. Pourquié, Large Eddy Simulation of an Ahmed reference model, J. Turbulence 3 (012) (2002). Institute of Physics Pub Ltd.
[13] A. Sohankar, C. Norberg, L. Davidson, Simulation of three-dimensional flow around a square cylinder at moderate Reynolds numbers, Phys. Fluids 11 (1999) 288–306.
[14] A.K. Saha, G. Biswas, K. Muralidar, Three-dimensional study of flow past a square cylinder at low Reynolds numbers, Int. J. Heat Fluid Flow 24 (2003) 54–66.
[15] A. Sohankar, L. Davidson, C. Norberg, Large eddy simulation on flow past a square cylinder: comparison of different subgridscale models, J. Fluid Eng. 122 (2000) 39–47.
[16] W. Rodi, J.H. Ferziger, M. Breuer, M. Pourquié, Status of large eddy simulation: results of a workshop, ASME J. Fluid Engrg. 119 (2) 119 (1997) 248–262.

[17] C.H.K. Williamson, Vortex dynamics in the cylinder wake, Annu. Rev. Fluid. Mech. 28 (1996) 477.
[18] M. Lesieur, O. Métais, New trends in large-eddy simulations of turbulence, Annu. Rev. Fluid. Mech. 28 (1996) 45–82.
[19] O. Métais, M. Lesieur, Spectral large-eddy simulation of isotropic and stably stratified turbulence, J. Fluid Mech. 239 (1992) 157–194.
[20] F. Ducros, P. Comte, M. Lesieur, Large-eddy simulation of transition to turbulence in a boundary layer developing spatially over a flat plate, J. Fluid Mech. 326 (1996) 1–36.
[21] J.L. Aider, A. Danet, Large-eddy simulation study of upstream boundary conditions influence upon a backward-facing step flow, C. R. Mecanique 334 (2006) 447–453.
[22] S. Laizet, E. Lamballais, Simulation numérique directe de l'influence de la forme aval d'une plaque séparatrice sur une couche de mélange, C. R. Mecanique 334 (2006) 454–460.
[23] I. Orlansky, A simple boundary condition for unbounded hyperbolic flows, J. Comp. Phys. 21 (1976) 251.
[24] Y. Dubief, F. Delcayre, On coherent vortex identification in turbulence, J. Turbulence 1 (011) (2000) 11.
[25] H. Djeridi, M. Braza, R. Perrin, G. Harran, E. Cid, S. Cazin, Near-wake turbulence properties around a circular cylinder at high Reynolds number, Flow, Turbulence and Combustion 71 (2003) 19–34.
[26] T. Goossens, Etude expérimentale et numérique du sillage turbulent et des forces instationnaires sur un obstacle bi-dimensionnel non profilé, PhD Thesis, Université d'Orléans, 2005.
[27] M. Lesieur, Turbulence in Fluids, third revised and enlarged edition, Kluwer Academic Publishers, 1997.
[28] M. Lesieur, O. Métais, P. Comte, Large-Eddy Simulations of Turbulence, Cambridge University Press, 2005.
[29] M. Braza, P. Chassaing, H. Ha Minh, Numerical study and physical analysis of the pressure and velocity fields in the near wake of a circular cylinder, J. Fluid Mech. 165 (1986) 79.
[30] A. Kourta, H.C. Boisson, P. Chassaing, H. Ha Minh, Non-linear interaction and the transition to turbulence in the wake of a circular cylinder, J. Fluid Mech. 181 (1987) 141.
[31] A. Prasad, C.H.K. Williamson, The instability of the shear layer separating from a bluff body, J. Fluid Mech. 333 (1997) 375.